

Doppler broadening and collisional relaxation effects in a lasing-without-inversion experiment

Martin Graf*

Max-Planck Institut für Quantenoptik, 85740 Garching, Germany

Ennio Arimondo†

Dipartimento di Fisica, Università di Pisa, 56100 Pisa, Italy

Edward S. Fry, Dmitri E. Nikonov, G. G. Padmabandu, Marlan O. Scully, and Shi-Yao Zhu
Texas Laser Laboratory, Houston Advanced Research Center, The Woodlands, Texas 77381
and Department of Physics, Texas A&M University, College Station, Texas 77843
 (Received 12 January 1995)

In the early experiments on optical pumping and coherent population trapping ("dark resonances") increasing buffer gas pressure enhances the effect. In our recent lasing-without-inversion experiments, based on population trapping, we find the opposite behavior, namely, decreasing atomic coherence with increasing buffer gas pressure. We provide a theoretical explanation of this result in agreement with experiment.

PACS number(s): 32.80.Bx, 34.50.-s, 42.55.-f

I. INTRODUCTION

In recent experiments in our laboratory [1], the influence of atomic coherence in optical pumping has been demonstrated, and amplification by stimulated emission without inversion [2] has been observed. In the present paper we investigate the effects of atomic collisions on these phenomena and find them to be surprisingly sensitive to buffer gas pressure. We present the experimental data and a theoretical analysis which is in agreement with our observations.

The experiment was carried out in a vapor cell with sodium as an active medium and helium as a buffer gas. Two circularly polarized phase correlated laser fields couple the ground states $S_{1/2}, F = 2$ and $S_{1/2}, F = 1$ of Na to the excited $P_{1/2}$ level. This leads to a coupling of ground-state pairs with the same magnetic quantum numbers to a common excited level and therefore to population trapping via atomic coherences [3]. The resonant coupling region depicted in Fig. 1 gives a simplified model for this system, where b' , b stand for the pair of levels within the hyperfine split $S_{1/2}$ sodium ground-state, coupled by two fields with frequencies ν_1, ν_2 to the common excited level a within the $P_{1/2}$ manifold. The level c is coupled to level a via spontaneous emission; e.g., in the case of right-circularly polarized (RCP) light the $S_{1/2}, F = 2, m = 2$ level could be the c state.

Only relaxation processes caused by collisions with the wall and other atoms might seem to be important for

population relaxation within the ground states and decay of coherence between them. This coherence is of special interest to us due to the crucial role of the atomic coherence in the lasing-without-inversion (LWI) experiments. However, velocity-changing collisions (VCC's) can be much more important than the longitudinal and transverse relaxation effects just mentioned.

In view of the importance of VCC's we divide the Doppler profile into two regions as in Fig. 1. In the central region both laser fields are strongly coupled to the atoms and ground-state coherence (which means population trapping) is important. In the wings of the Doppler profile, on the other hand, only one hyperfine level has a proper Doppler velocity subgroup leading to laser absorption. In this region no ground-state coherence can develop, and only "rate equation" optical pumping is involved. The effect of VCC's in shuffling atoms between these regions will be seen to be very important to the present experiments.

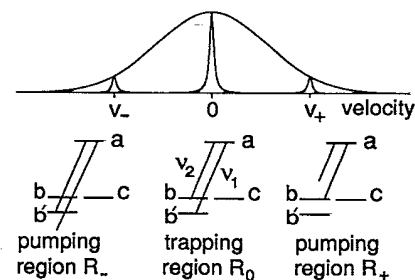


FIG. 1. (a) Schematic representation of the atomic velocity distribution with relevant velocity groups around zero, v_+ and v_- . (b) Schematic description of the various coupling schemes at the different velocity regions of the Maxwell distribution.

*Present address: Walter Schottky Institut, TU München, 85748 Garching, Germany.

†Present address: JILA, University of Colorado, Boulder, CO 80309-0440.

II. RELAXATION IN OPTICAL PUMPING WITH A SINGLE FIELD

We will consider two cases: (1) optical pumping with a broadband light source that can resonantly excite all atoms under the Doppler profile, and (2) optical pumping with a narrow-band light source that is resonant with only a small segment of atoms under the Doppler profile. For a broadband source of light (e.g., a lamp), one contribution to relaxational effects is due to collisions with the walls of the vapor cell [4,5] having radius R_c . In the case of uncoated walls one assumes that such a collision causes a randomization within the ground-state magnetic sublevels. The process of atoms moving to the wall and coming back "fresh" is described in a density-matrix equation by the injection of atoms with an equal ground-state population distribution having no coherence between them. Its rate is determined by the time of flight through the cell in the absence of atomic collisions. When a buffer gas is added, this relaxation time is determined by a random walk diffusive process. The rate for the combination of the diffusion and the free-flight processes is given by Ref. [6] as

$$r_{\text{wall}} = \frac{(2.405)^2 D}{R_c^2} \left(\frac{1}{1 + cK} \right), \quad (1)$$

where D is the diffusion coefficient proportional to the mean free path $\lambda \propto p^{-1}$, p is the buffer gas pressure, $c = 6.8$ in the hard sphere limit for the collision process, and K is the Knudsen number $K = \lambda/R_c$.

Figure 2 shows important rates for optical and coherence pumping as a function of buffer gas pressure, where we will use the term "coherence pumping" if coherence effects are of crucial importance. In the case of pumping with the broadband, incoherent light source there is no velocity selectivity and VCC's are not important, i.e., the relaxation rate is given solely by r_{wall} .

However, in the case of optical pumping with a laser, i.e., a narrow-band coherent light source, increasing the buffer gas pressure leads to VCC's which take the atoms out of the resonance region before they hit the wall. Hence this is another process for the loss of atoms from

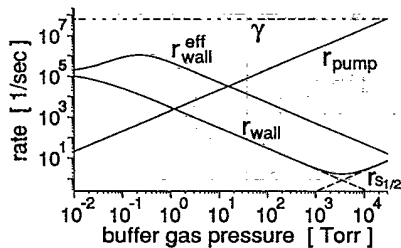


FIG. 2. Relevant rates for the Na-He system: r_{wall} , population relaxation due to diffusion to the wall; $r_{\text{wall}}^{\text{eff}}$, effective population relaxation due to wall collisions for the case of narrow-band excitation light; r_{pump} , effective injection of pumped atoms due to the action of the fields in the velocity regions v_+ and v_- . Shown for comparison are the radiative decay γ and the spin-flip relaxation rate $r_{S_{1/2}}$ in the $S_{1/2}$ ground-states.

the resonant region. In a typical cell experiment, the nonresonant region in the Maxwell velocity distribution contains many more atoms than the resonant one and acts as a kind of reservoir. Resonant Na atoms that, through VCC's, are scattered into the nonresonant region, have some probability to be scattered back into the resonant region. This "reservoir" circulation of the Na atoms modifies the relaxation rate for the resonant atoms produced by the collisions with the buffer gas. In the limit of an optical pumping rate larger than both the VCC rate r_{coll} and the wall relaxation r_{wall} , a rate equation calculation gives an effective rate for the diffusion injection of "fresh" atoms from the wall into the resonant region (or equivalently the effective rate for the loss of optically pumped atoms from the resonant region)

$$r_{\text{wall}}^{\text{eff}} = r_{\text{wall}} \frac{r_{\text{wall}} + r_{\text{coll}}}{r_{\text{wall}} + r_{\text{coll}} n_0/n}, \quad r_{\text{coll}} = n_{\text{He}} \sigma_{\text{coll}} \bar{v}. \quad (2)$$

This rate, which is derived in Appendix A, applies to atoms in the resonant region [7]. In Eq. (2) n_0/n is the ratio of resonant to total Na density, n_{He} is the He buffer gas density, σ_{coll} is the gas kinetic cross section, and \bar{v} is the average relative velocity of Na and He. Modeled this way, the only difference at higher buffer gas pressures between broadband and narrow-band optical pumping is the factor n/n_0 which leads to an enhanced effective wall collision relaxation rate (Fig. 2) in the narrow-band case. This is also essentially valid for two uncorrelated laser beams, the linewidths of which are such that they are not able to produce ground-state coherences.

In Eq. (2), the transverse and longitudinal relaxation effects due to atom-atom collisions have been neglected. This is reasonable because the ground-state of the alkali-metal atoms is an S state, and the buffer gas atoms (He) have a stable closed shell with only high lying excited levels. Specifically, the collisional processes leading to coherence and population relaxation in collisions are due to a modification of the hyperfine interaction and spin-orbit coupling of the Na spin, resulting in a spin flip [8]. These are very weak processes, involving cross sections $\sigma_{\text{pop}} \approx 10^{-26} \text{ cm}^2$ for the population relaxation and $\sigma_{\text{coh}} \approx 10^{-24} \text{ cm}^2$ for the coherence decay [9]. These are to be compared with the gas kinetic cross section $\sigma_{\text{coll}} \approx 10^{-15} \text{ cm}^2$. The corresponding rates are proportional to the buffer gas pressure, e.g., the typical population relaxation rate is $r_{S_{1/2}} = n_{\text{He}} \sigma_{\text{pop}} \bar{v}$. The spin-orbit-coupling relaxation for the ground-states ($S_{1/2}$ spin-flip process), shown in Fig. 2, is much less important than wall collisions in the buffer gas pressure range of the experiments ($p < 100 \text{ Torr}$) [10].

III. VELOCITY-CHANGING COLLISIONS AND DOPPLER BROADENING

One effect of the Doppler frequency shift in optical pumping with a narrow-band frequency source, such as a laser, has already been described above: only a small fraction of the atoms is in the velocity subgroup which

is resonant with the field; most of the population is a kind of reservoir. Now consider the case of two laser beams, which are both on resonance, i.e., their frequency difference is that of the ground-state hyperfine splitting. One might expect less diffusive relaxation and therefore a better coherence as the buffer gas pressure increases. However, consider a velocity group having a Doppler frequency shift of the order of the ground-state hyperfine splitting. The field, which for zero velocity atoms was resonant with $b' \leftrightarrow a$, can now couple b and a due to the Doppler shift (see pumping region R_+ in Fig. 1). Atoms in this velocity group will thus be affected by only one field, which leads to destruction of the b, b' coherence by rate equation optical pumping of the atoms out of states b and c . Such effects occur at velocities $v_{\pm} = \lambda_{D_1} \Delta_{\text{hf}}$ (here $v_{\pm} = \pm 1043$ m/s) where Δ_{hf} is the ground-state hyperfine splitting (in Na 1.77 GHz) and λ_{D_1} is the wavelength of the D_1 line (589.5 nm).

The populations of these two regions, R_+ and R_- (Fig. 1), relative to the whole Na population are quite small. For the above mentioned velocities and with the laser linewidth of the order of the radiative linewidth, approximately 10^{-4} of the total sodium concentration is in regions R_+ and R_- . But this is large enough to explain the observed dependence of the coherence on buffer gas pressure, because in these regions of the population "reservoir" optical pumping takes place and "kills" the coherence. We assume a strong enough laser field and short enough upper state lifetime for complete optical pumping (and therefore coherence quenching) during the interaction time (the time between successive VCC's is equal to r_{coll}^{-1}). Thus this process goes linearly with pressure, and is important when the associated injection of optically pumped "quenched" atoms into the zero velocity (central resonant) region exceeds the rate of diffusion injection of "fresh" zero velocity atoms from the wall. The effective rate r_{pump} (Fig. 2) for this quenching of atoms by optical pumping is caused by the single field action on the populations in the detuned regions around v_+ and v_- ; the entire population continuously shuffles

through these regions due to VCC's.

This optical pumping can be regarded as injecting atoms into level c , which is not coupled to the laser fields. Even when the atoms return to the central resonant region, if they are in the state c they cannot be affected by the fields, so the coherent trapping by the joint action of the fields cannot be created. At pressures larger than several Torr, this injection of "pumped" atoms overwhelms that of "fresh" atoms from wall collisions. (The wall collisions return atoms in any state as "fresh" atoms that the *can be* brought into the trapping state.) At significantly larger pressures, the population is collected by optical pumping to state c and atoms do not exhibit population trapping in the $b-b'$ pair.

IV. RELAXATION IN LASING WITHOUT INVERSION

We now turn from the above qualitative discussion to the appropriate calculations which model the physics. We describe the role of collisions via a density-matrix equation of motion for the Na atoms by a collision kernel $W_{ij}(v' \rightarrow v)$, which gives the rate of collisions for atoms with velocity v' scattering to velocity v for the various density-matrix elements $\rho_{ij}(v')$ which describe these atoms [11,12]. As we are in a regime (buffer gas pressure $p \ll 100$ Torr) where the collision rate is smaller than the decay rate γ of the excited level a , we can assume that the collision kernel is approximately the same for all populations and ground-state coherences. Now one can transform the density-matrix equation in an interaction representation for each of the three different velocity regions of Fig. 1. This permits a rotating wave approximation.

Straightforward calculation along the lines of Ref. [11], given in Appendix B, leads us to define the vector $P(v, t)$ for the populations $\rho_{\alpha\alpha}$ ($\alpha = a, b, b'$) and the real $\text{Re}\rho_{\alpha\beta}$ and imaginary $\text{Im}\rho_{\alpha\beta}$ components of the density matrix

$$P(v, t) = [\rho_{aa}, \rho_{bb}, \rho_{b'b'}, \text{Re } \tilde{\rho}_{ab}, \text{Im } \tilde{\rho}_{ab}, \text{Re } \tilde{\rho}_{ab'}, \text{Im } \tilde{\rho}_{ab'}, \text{Re } \tilde{\rho}_{bb'}, \text{Im } \tilde{\rho}_{bb'}]^T. \quad (3)$$

We find that Eq. (3) obeys the equation of motion

$$\dot{P}(v, t) = \int dv' \mathbf{B}(v', v) P(v', t) + \mathbf{C}(v) - \mathbf{A}(v) P(v, t), \quad (4)$$

where $\mathbf{A}(v)$ contains the action of the fields, the dissipative decay phenomena and loss due to VCC's. For the central region $|v| < c\Delta_{\text{hf}}/(2\nu_{D_1})$ (we have drawn the border in the middle between the resonance regions)

$$\mathbf{A}(v) = \begin{bmatrix} \gamma + \Gamma_0(v) & 0 & 0 & 0 & -2\Omega_2 & 0 & -2\Omega_1 & 0 & 0 \\ -\gamma/3 & \Gamma_0(v) & 0 & 0 & 2\Omega_2 & 0 & 0 & 0 & 0 \\ -\gamma/3 & 0 & \Gamma_0(v) & 0 & 0 & 0 & 2\Omega_1 & 0 & 0 \\ 0 & 0 & 0 & \gamma'_{ab}(v) & -\Delta_2(v) & 0 & 0 & 0 & -\Omega_1 \\ \Omega_2 & -\Omega_2 & 0 & \Delta_2(v) & \gamma'_{ab}(v) & 0 & 0 & -\Omega_1 & 0 \\ 0 & 0 & 0 & 0 & 0 & \gamma'_{ab'}(v) & -\Delta_1(v) & 0 & \Omega_2 \\ \Omega_1 & 0 & -\Omega_1 & 0 & 0 & \Delta_1(v) & \gamma'_{ab'}(v) & -\Omega_2 & 0 \\ 0 & 0 & 0 & 0 & \Omega_1 & 0 & \Omega_2 & \gamma'_{bb'}(v) & \Delta_{bb'}(v) \\ 0 & 0 & 0 & \Omega_1 & 0 & -\Omega_2 & 0 & -\Delta_{bb'} & \gamma'_{bb'}(v) \end{bmatrix}. \quad (5)$$

where $\Delta_1(v) = \omega_1 - \nu_1(1 - v/c)$, $\Delta_2(v) = \omega_2 - \nu_2(1 - v/c)$, and $\Delta_{bb'} = \Delta_2 - \Delta_1$ are the detunings, ω_1 corresponds to the energy of the $a \leftrightarrow b'$ transition and ω_2 to the $a \leftrightarrow b$ transition. The Rabi frequencies are defined by $\Omega_i = \mathcal{E}_i \rho_i / \hbar$ where ρ_i are the dipole matrix elements for the optical transitions and \mathcal{E}_i are the fields coupling these transitions ($i = 1, 2$). The decay rate of the optical transitions is γ ; for the collision rate $\Gamma(v)$ at velocity v and the wall relaxation r_{wall} we have used the rates

$$\begin{aligned} \Gamma(v) &= \int dv' r_{\text{coll}} W(v \rightarrow v'), \\ \Gamma_0(v) &= \Gamma(v) + r_{\text{wall}}, \\ \gamma'_{bb'}(v) &= \Gamma(v) + r_{\text{wall}} + \gamma_{bb'}^{\text{phase}}(v), \\ \gamma'_{aj}(v) &= \gamma/2 + \Gamma(v) + r_{\text{wall}} \text{ for } j = b, b'. \end{aligned} \quad (6)$$

With the above stated approximations for the normalized collision kernel W , the only nonzero elements of the matrix $\mathbf{B}(v', v)$, which yields the population and ground-state coherence transfer by VCC's, are

$$B_{1,1} = B_{2,2} = B_{3,3} = B_{8,8} = B_{9,9} = r_{\text{coll}} W(v' \rightarrow v). \quad (7)$$

The vector $\mathbf{C}(v)$ describes the injection of fresh atoms due to wall collisions, where the only nonzero elements are $C_2(v) = C_3(v) = F(v) r_{\text{wall}}/3$ and $F(v)$ is the Maxwell velocity distribution. These two elements correspond to atoms being injected in levels b and b' .

For the other velocity regions R_+ and R_- there exist similar matrices $\mathbf{A}(v)$, obtained by considering the different coupling schemes and modified detunings and Rabi frequencies.

With the further assumption of strong collisions, i.e., $W(v' \rightarrow v) = F(v)$, Eq. (4) can easily be solved for the steady state solution of $P(v)$ in the case of constant laser fields, leading to

$$\begin{aligned} P(v) &= \mathbf{A}^{-1}(v) \mathbf{B}(0, v) \left[1 - \int dv'' \mathbf{A}^{-1}(v'') \mathbf{B}(0, v'') \right]^{-1} \\ &\times \int dv' \mathbf{A}^{-1}(v') \mathbf{C}(v') + \mathbf{A}^{-1}(v) \mathbf{C}(v). \end{aligned} \quad (8)$$

The numerical results of this calculation are shown in Figs. 3 and 4 by using the parameters from our experi-

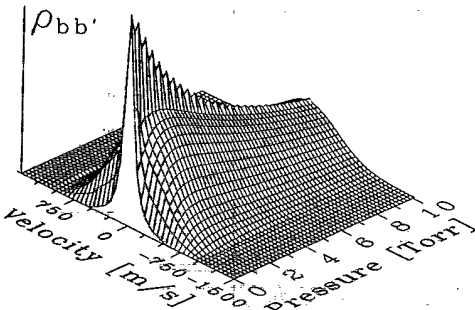


FIG. 3. Velocity and pressure dependence of the ground-state coherence $P_8(v) = \text{Re} \tilde{\rho}_{bb'}$.

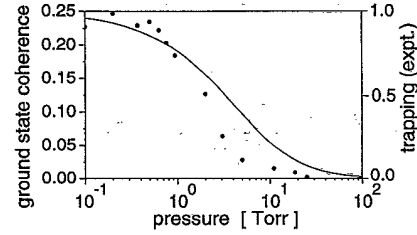


FIG. 4. The ground-state coherence $P_8(v = 0) = \text{Re} \tilde{\rho}_{bb'}(v = 0)$ as a function of buffer gas pressure: the numerical result (solid curve) and the experimental result (data points) [10].

ment (Ref. [1]) and summarized in Table I. In Fig. 3 we show the velocity distribution and pressure dependence of the ground-state coherence $P_8(v) = \text{Re} \tilde{\rho}_{bb'}(v)$. In Fig. 4 the ground-state coherence $P_8(v = 0) = \rho_{bb'}(v = 0)$ for the “resonant” atoms is shown. This is measured experimentally by utilizing fast pulses (much shorter than the time scale of VCC's). For comparison we show the experimental result for the ground-state coherence in Fig. 4 ([10]). There is good agreement with our simple four-level model, showing the decrease of coherence effects at a few Torr of buffer gas.

V. DISCUSSION

A more exact calculation would require an analysis considering all 16 levels of the sodium D_1 manifold, with a collisional coupling to the $P_{3/2}$ levels and the use of a more sophisticated kernel (e.g., without the strong collision approximation) [6]. Also, in a multilevel model, the inclusion of scattering of the excited-state coherence by VCC's across the whole velocity distribution (similar to [13]) would be necessary. This calculation is underway. We emphasize, however, that the present “simple” model explains the physics of the process quite well.

In conclusion we consider the difference between our work and other experiments on establishing coherence in which the dependence on the buffer gas pressure was similar to that of optical pumping. In the early experiment of Alzetta *et al.* [14], trapping effects in an optical pumping experiment within the Na D_1 line were observed; however, no significant dependence on buffer gas pressure was reported. The reason is due to the fact that they used a multimode laser with many modes oscillating at equally spaced frequencies. For the point in space where

TABLE I. Values for the parameters used for numerical simulation of the experiment.

Parameter	Value
$\Delta\nu_{\text{Dop}}$	$2\pi \times 1.6$ GHz
γ	$2\pi \times 9.9$ MHz
$\Omega_1, \Omega_2, \Omega_3$	$\approx \gamma$
r_{wall}	$\gamma/(125 + 360 p$ [Torr])
r_{coll}	γ 0.1 p [Torr]
γ^{phase}	0

the dark resonance was observed the frequency difference between the n th and the $(n+5)$ th modes was equal to the splitting between the lower hyperfine sublevels. Thus for each velocity group under the Doppler profile, one could always find a pair of laser modes that couple the two lower sublevels to the same upper sublevel. Thus, unlike our experiment, there were no velocity groups where coherence trapping of a newly arrived atom would be depleted by optical pumping. For this case the population trapping is limited by the ratio of the collision rate $r_{\text{wall}}^{\text{eff}}$ to the radiative decay rate rather than to the r_{pump} rate.

In a more recent version of that experiment [15], ground-state population trapping has been produced using a three-mode dye laser in which the frequency separation between adjacent modes matched the sodium ground-state hyperfine splitting. Even though that pump configuration is a close approximation to that of our experiment, no significant decrease in coherent population trapping with the buffer gas pressure was observed, at least for the pressure range explored in Figs. 3 and 4. In the experiments of Refs. [14] and [15] one choice of the hyperfine levels b' and b was the states $F = 2, m_F = -2$ and $F = 1, m_F = -1$, respectively. With this level choice, the addition of buffer gas together with the optical pumping actually produced an enhancement of population in the b level involved in the coherent trapping superposition. This dependence on buffer gas pressure is opposite to that observed in our work in which optical pumping produced by the addition of buffer gas depletes the population of both levels involved in the trapping superposition.

The explanation is found in another significant difference in the experiments of Refs. [14] and [15]. Specifically, the laser beam is left-circularly polarized and propagates along the axis of the cell, whereas there is a relatively strong magnetic field at an angle α from 20° to 40° to the axis of the cell. Using the magnetic field as the quantization axis, the pure left-circularly polarized light propagating at an angle α would in this representation have a linear polarization component that drives $\Delta m_F = 0$ transitions. Thus atoms in the $m_F = -2$ state could be affected by this field and could produce population trapping in their $F = 2, m_F = -2$ and $F = 1, m_F = -1$ combinations. In this configuration there is no longer a state to which all the atoms can be pumped and which is not affected by any field. Thus VCC's cannot move all the atoms in an inaccessible state. It should also be noted that if $\alpha = 0$, the $F = 2, m_F = -2$ and $F = 1, m_F = -1$ coherence disappears. But they do still observe an $F = 2, m_F = -1$ and $F = 1, m_F = -1$ coherence that is analogous to the one we observe. We anticipate that with $\alpha = 0$ and two laser modes, buffer gas pressure dependence of this coherence would be similar to our observations.

ACKNOWLEDGMENTS

This work was supported by the Office of Naval Research, the Welch Foundation, and the Texas Advanced Research Program.

APPENDIX A: EFFECTIVE RELAXATION RATE

In the case of optical pumping with a narrow-band light source, e.g., a laser, increasing the buffer gas pressure leads to collisions which take the atoms out of the resonant region even before they leave the light beam. At the temperatures of interest, the nonresonant region in the Maxwell velocity distribution contains many more atoms than the resonant region, thus it acts as a kind of reservoir. An increase of the collision rate leads to a higher flux of atoms out of the resonant region. Specifically, the concentration of optically pumped atoms that have been scattered into another velocity group grows, and so does the probability for them to scatter back into the resonant velocity region without diffusing to, and relaxing at, the wall. Let us express the above reasoning in terms of rate equations; the contributions to the processes are proportional to the following number densities.

- (i) n : Total concentration of Na atoms ($n = n_0 + n_{\text{res}}$).
- (ii) n_0 : Concentration of Na atoms in the resonant region ($n_0 \ll n$).
- (iii) n_{res} : Concentration of Na atoms in the reservoir region ($n_{\text{res}} \approx n$).
- (iv) n^p : Concentration of optically pumped Na atoms in one of the two regions.
- (v) n^f : concentration of "fresh" Na atoms in one of the two regions.

The total concentrations both in the resonant region $n_{\text{res}} = n_{\text{res}}^f + n_{\text{res}}^p$ and the reservoir region $n_0 = n_0^f + n_0^p$ are constant, so we will only write equations for pumped atoms in the resonant region n_{res}^p and pumped atoms in the reservoir n_0^p . The process of escape of pumped atoms to the walls and return of fresh atoms is described by the terms with the rate r_{wall} times the concentrations of pumped atoms. In the resonant region fresh atoms are being pumped with the rate R due to the laser field. We assume that the pumping rate is sufficiently high that the atoms undergo complete pumping (the equilibrium of the radiative processes is achieved) before they scatter again. The equations have the form

$$\dot{n}_0^p = R(n_0 - n_0^p) - r_{\text{wall}}n_0^p - r_{\text{coll}}\frac{n - n_0}{n}n_0^p + r_{\text{coll}}\frac{n_0}{n}n_{\text{res}}^p, \quad (\text{A1})$$

$$\dot{n}_{\text{res}}^p = -r_{\text{wall}}n_{\text{res}}^p + r_{\text{coll}}\frac{n - n_0}{n}n_0^p - r_{\text{coll}}\frac{n_0}{n}n_{\text{res}}^p. \quad (\text{A2})$$

The last two terms in each equation are due to the collisional transfer of atoms via VCC's with the buffer gas from the resonant region to the reservoir and vice versa, respectively. The weighting factor n_0/n describes the probability that an atom which has experienced a collision in the reservoir region will be scattered into the resonant region, and $n - n_0/n$ describes the reverse.

If we assume that the pumped atom concentration in the reservoir is constant in the steady state (i.e., $\dot{n}_{\text{res}}^p = 0$), then the second equation, Eq. (A2), gives

$$n_{\text{res}}^p = \frac{r_{\text{coll}}n_0^p(n - n_0)/n}{r_{\text{wall}} + r_{\text{coll}}n_0/n}. \quad (\text{A3})$$

We now define $r_{\text{wall}}^{\text{eff}}$ to be an effective rate for the escape of a pumped atom to the wall, or equivalently, the effective rate for the appearance of a fresh atom in the resonant region. Then we have

$$\dot{n}_0^p = R(n_0 - n_0^p) - r_{\text{wall}}^{\text{eff}} n_0^p. \quad (\text{A4})$$

By substituting Eq. (A3) into Eq. (A1), and comparing with Eq. (A4), we find

$$r_{\text{wall}}^{\text{eff}} = r_{\text{wall}} \frac{r_{\text{wall}} + r_{\text{coll}}}{r_{\text{wall}} + r_{\text{coll}} n_0 / n}. \quad (\text{A5})$$

This rate can be used in the density-matrix equation written for only one velocity group to take into account some effects of Doppler broadening.

APPENDIX B: DERIVATION OF THE KINETIC EQUATION

To study the influence of velocity-changing collisions we need to add the dependence on the velocity to the density-matrix equation and the terms describing the exchange due to collisions. We will approximate the collision integral by the collision kernel $W_{ij}(v' \rightarrow v)$ which gives the rate of collisions for atoms with velocity v' which lead to a transfer to velocity v for the various density-matrix elements $\rho_{ij}(v')$ which describe these atoms [11]. As we are interested in a low pressure regime where the decay rate γ at the optical D_1 transition line is much larger than the gas-kinetic collision rate, the transport of coherence in the optical transition, i.e., polarization, from one velocity group to another is here of no importance, especially as the cross section for population and coherence decay by buffer gas collisions within the $P_{1/2}$ manifold is of the order of the gas-kinetic cross-section. For the ground-state coherence there is a different situation, as the effective ground-state relaxation (i.e., including the wall relaxation) becomes smaller than the collision rate with increasing buffer gas pressure. Therefore it cannot be neglected. We neglect the transverse relaxation in comparison with the change of state which is longitudinal relaxation. So we assume the same collision kernels for the following elements of the density matrix:

$$\begin{aligned} W_{aa}(v \rightarrow v') &= W_{bb}(v \rightarrow v') \\ &= W_{b'b'}(v \rightarrow v') \\ &= W_{cc}(v \rightarrow v') \\ &= r_{\text{coll}} W(v \rightarrow v'), \\ W_{bb'}(v \rightarrow v') &= W_{bc}(v \rightarrow v') = W_{b'c}(v \rightarrow v') \\ &= r_{\text{coll}} W(v \rightarrow v'), \\ W_{ab}(v \rightarrow v') &= W_{ab'}(v \rightarrow v') = W_{ac}(v \rightarrow v') = 0. \end{aligned} \quad (\text{B1})$$

Here the kernel $W(v \rightarrow v')$ is normalized to the equilibrium Maxwell distribution $F(v)$:

$$1 = \int \int dv dv' F(v) W(v \rightarrow v'). \quad (\text{B2})$$

The velocity-dependent rate of collisions $\Gamma(v)$ of atoms

with a certain velocity v results then in

$$\Gamma(v) = \int dv' r_{\text{coll}} W(v \rightarrow v'). \quad (\text{B3})$$

Using a term $\gamma_{ij}^p(v)$ for an additional phase decay caused by spin-angular-momentum coupling in the alkali-metal-buffer-gas interaction, the collisional part of the equation of motion for the density matrix can be written as

$$\begin{aligned} \left[\frac{\partial}{\partial t} \rho_{ij}(z, v, t) \right]_{\text{coll}} &= -\gamma_{ij}^p(v) \rho_{ij}(z, v, t) \\ &\quad - \Gamma(v) \rho_{ij}(z, v, t) \\ &\quad + \int dv' W_{ij}(v' \rightarrow v) \rho_{ij}(z, v', t). \end{aligned} \quad (\text{B4})$$

The dependence on z is important for the transition to the rotating frame of reference.

For the resonant region, i.e., where the field with the frequency ν_1 couples the transition $a \leftrightarrow b'$ and the field with ν_2 couples $a \leftrightarrow b$ and the wave vectors are K_1 and K_2 respectively, this representation is given by

$$\begin{aligned} \rho_{ab}(z, v, t) &= \tilde{\rho}_{ab}(v, t) e^{i[K_2 z - \nu_2 t]}, \\ \rho_{ab'}(z, v, t) &= \tilde{\rho}_{ab'}(v, t) e^{i[K_1 z - \nu_1 t]}, \\ \rho_{bb'}(z, v, t) &= \tilde{\rho}_{bb'}(v, t) e^{i[(K_1 - K_2)z - (\nu_1 - \nu_2)t]}. \end{aligned} \quad (\text{B5})$$

For the region where the field with the frequency ν_1 is coupled to the transition $a \leftrightarrow b$ (i.e., for atoms with a velocity around v_-) we choose

$$\begin{aligned} \rho_{ab}(z, v, t) &= \tilde{\rho}_{ab}(v, t) e^{i[K_1 z - \nu_1 t]}, \\ \rho_{ab'}(z, v, t) &= \tilde{\rho}_{ab'}(v, t) e^{i[(2K_1 - K_2)z - (2\nu_1 - \nu_2)t]}, \\ \rho_{bb'}(z, v, t) &= \tilde{\rho}_{bb'}(v, t) e^{i[(K_1 - K_2)z - (\nu_1 - \nu_2)t]}, \end{aligned} \quad (\text{B6})$$

where we have chosen the rotating frame for the uncoupled $a \leftrightarrow b'$ transition in such a way that the $\rho_{bb'}$ element has in both regions the same decomposition. This leads to a time-independent right hand side in Eq. (B7) below. The formulation for the velocity around v_+ is similar. For convenience of calculation, we assume that we switch from one coupling scheme to another at the velocity corresponding to the detuning $\Delta_{\text{hf}}/2$ of the fields, and that there is no significant difference between both schemes at this point since the fields are too far detuned. If this were not valid, one would have to work with the more accurate description of both fields coupling both transitions simultaneously, which would lead to time-dependent terms oscillating with frequencies Δ_{hf} and higher harmonics, as there is no rotating frame for this set of equations. The density-matrix equations for the resonant region are now

$$\begin{aligned}
\frac{d}{dt}\rho_{aa}(v, t) &= -[\gamma + \Gamma(v) + r_{\text{wall}}]\rho_{aa}(v, t) + i\Omega_2\tilde{\rho}_{ba} + i\Omega_1\tilde{\rho}_{b'a} - i\Omega_2^*\tilde{\rho}_{ab} - i\Omega_1^*\rho_{ab'} + \int dv' r_{\text{coll}}W(v' \rightarrow v)\rho_{aa}(v', t), \\
\frac{d}{dt}\rho_{bb}(v, t) &= r_{\text{wall}}/3 F(v) + \gamma/3 \rho_{aa}(v, t) - [\Gamma(v) + r_{\text{wall}}]\rho_{bb}(v, t) - i\Omega_2\tilde{\rho}_{ba} + i\Omega_2^*\tilde{\rho}_{ab} + \int dv' r_{\text{coll}}W(v' \rightarrow v)\rho_{bb}(v', t), \\
\frac{d}{dt}\rho_{b'b'}(v, t) &= r_{\text{wall}}/3 F(v) + \gamma/3 \rho_{aa}(v, t) - [\Gamma(v) + r_{\text{wall}}]\rho_{b'b'}(v, t) - i\Omega_1\tilde{\rho}_{b'a} + i\Omega_1^*\tilde{\rho}_{ab'} \\
&\quad + \int dv' r_{\text{coll}}W(v' \rightarrow v)\rho_{b'b'}(v', t), \\
\frac{d}{dt}\rho_{cc}(v, t) &= r_{\text{wall}}/3 F(v) + \gamma/3 \rho_{aa}(v, t) - [\Gamma(v) + r_{\text{wall}}]\rho_{cc}(v, t) + \int dv' r_{\text{coll}}W(v' \rightarrow v)\rho_{cc}(v', t), \\
\frac{d}{dt}\tilde{\rho}_{ab}(v, t) &= -[\gamma/2 + \gamma_{ab}^p + \Gamma(v) + r_{\text{wall}} + i\Delta_2(v)]\tilde{\rho}_{ab}(v, t) - i\Omega_2(\rho_{aa} - \rho_{bb}) + i\Omega_1\tilde{\rho}_{b'b}, \\
\frac{d}{dt}\tilde{\rho}_{ab'}(v, t) &= -[\gamma/2 + \gamma_{ab'}^p + \Gamma(v) + r_{\text{wall}} + i\Delta_1(v)]\tilde{\rho}_{ab'}(v, t) - i\Omega_1(\rho_{aa} - \rho_{b'b'}) + i\Omega_2\tilde{\rho}_{bb'}, \\
\frac{d}{dt}\tilde{\rho}_{bb'}(v, t) &= -[\gamma/2 + \gamma_{bb'}^p + \Gamma(v) + r_{\text{wall}} - i\Delta_{bb'}(v)]\tilde{\rho}_{bb'}(v, t) + i\Omega_2^*\tilde{\rho}_{ab'} - i\Omega_1\tilde{\rho}_{ba} + \int dv' r_{\text{coll}}W(v' \rightarrow v)\tilde{\rho}_{bb'}(v', t).
\end{aligned} \tag{B7}$$

The coherence terms involving the level c are zero, as no fields couple to this transition and there is no injected coherence. The detunings are $\Delta_1(v) = \omega_1 - \nu_1 + K_1v$, $\Delta_2(v) = \omega_2 - \nu_2 + K_2v$, and $\Delta_{bb'} = \Delta_2 - \Delta_1$ where ω_1 corresponds to the energy of the $a \leftrightarrow b'$ transition and ω_2 to the $a \leftrightarrow b$ transition. The Rabi frequencies are defined by

$$\Omega_i = \frac{\mathcal{E}_i \rho_i}{\hbar}, \quad i = 1, 2, \tag{B8}$$

where ρ_i are the dipole matrix elements for the optical transitions and \mathcal{E}_i are the fields coupling these transitions.

For the detuned region around v_+ , we have

$$\begin{aligned}
\frac{d}{dt}\rho_{aa}(v, t) &= -[\gamma + \Gamma(v) + r_{\text{wall}}]\rho_{aa}(v, t) + i\tilde{\Omega}_1\tilde{\rho}_{ba} - i\tilde{\Omega}_1^*\tilde{\rho}_{ab} + \int dv' r_{\text{coll}}W(v' \rightarrow v)\rho_{aa}(v', t), \\
\frac{d}{dt}\rho_{bb}(v, t) &= r_{\text{wall}}/3 F(v) + \gamma/3 \rho_{aa}(v, t) - [\Gamma(v) + r_{\text{wall}}]\rho_{bb}(v, t) - i\tilde{\Omega}_1\tilde{\rho}_{ba} + i\tilde{\Omega}_1^*\tilde{\rho}_{ab} + \int dv' r_{\text{coll}}W(v' \rightarrow v)\rho_{bb}(v', t), \\
\frac{d}{dt}\rho_{b'b'}(v, t) &= r_{\text{wall}}/3 F(v) + \gamma/3 \rho_{aa}(v, t) - [\Gamma(v) + r_{\text{wall}}]\rho_{b'b'}(v, t) + \int dv' r_{\text{coll}}W(v' \rightarrow v)\rho_{b'b'}(v', t), \\
\frac{d}{dt}\rho_{cc}(v, t) &= r_{\text{wall}}/3 F(v) + \gamma/3 \rho_{aa}(v, t) - [\Gamma(v) + r_{\text{wall}}]\rho_{cc}(v, t) + \int dv' r_{\text{coll}}W(v' \rightarrow v)\rho_{cc}(v', t), \\
\frac{d}{dt}\tilde{\rho}_{ab}(v, t) &= -[\gamma/2 + \gamma_{ab}^p + \Gamma(v) + r_{\text{wall}} + i\tilde{\Delta}_1(v)]\tilde{\rho}_{ab}(v, t) - i\tilde{\Omega}_1(\rho_{aa} - \rho_{bb}), \\
\frac{d}{dt}\tilde{\rho}_{ab'}(v, t) &= -[\gamma/2 + \gamma_{ab'}^p + \Gamma(v) + r_{\text{wall}} + i\tilde{\Delta}_2(v)]\tilde{\rho}_{ab'}(v, t) + i\tilde{\Omega}_1\tilde{\rho}_{bb'}, \\
\frac{d}{dt}\tilde{\rho}_{bb'}(v, t) &= -[\gamma/2 + \gamma_{bb'}^p + \Gamma(v) + r_{\text{wall}} - i\Delta_{bb'}(v)]\tilde{\rho}_{bb'}(v, t) + i\tilde{\Omega}_1^*\tilde{\rho}_{ab'} + \int dv' r_{\text{coll}}W(v' \rightarrow v)\tilde{\rho}_{bb'}(v', t).
\end{aligned} \tag{B9}$$

Here the detunings are $\tilde{\Delta}_1(v) = \Delta_1(v) - \Delta_{\text{hf}}$ and $\tilde{\Delta}_2(v) = \Delta_2(v) - 2(1 - v/c)\delta\nu$; and the Rabi frequency is

$$\tilde{\Omega}_1 = \frac{\mathcal{E}_1 \rho_2}{\hbar}. \tag{B10}$$

These equations written in the matrix form give Eqs. (4)–(7).

- [1] E. S. Fry *et al.*, Phys. Rev. Lett. **70**, 3235 (1993).
[2] O. Kocharovskaya and Ya. I. Khanin, Pis'ma Zh. Eksp. Teor. Fiz. **48**, 581 (1988) [JETP Lett. **48**, 630 (1988)]; S. E. Harris, Phys. Rev. Lett. **62**, 1033 (1989); M. O. Scully, S.-Y. Zhu, and A. Gavrielides, *ibid.* **62**, 2813 (1989).

- [3] D. E. Nikonov *et al.*, Quantum Opt. **6**, 245 (1994).
[4] R. A. Bernheim, *Optical Pumping* (Benjamin, New York, 1965).
[5] W. Happer, Rev. Mod. Phys. **44**, 169 (1972), and references therein.
[6] J. E. M. Haverkort *et al.*, Phys. Rev. A **38**, 4054 (1988).

- [7] The derivation of this equation is in the spirit of P. G. Pappas *et al.*, *Phys. Rev. Lett.* **47**, 236 (1981).
- [8] J. Vanier and C. Audoin, *The Quantum Physics of Atomic Frequency Standards* (Adam Hilger, Bristol, 1989), Vol. 1.
- [9] The relaxation rates are from [8], where the rate for the coherence decay has been scaled by comparing Rb-He with Na-He collisions, since the underlying physical processes are the same for these.
- [10] G. G. Padmabandu *et al.*, *Quantum Opt.* **6**, 261 (1994).
- [11] A. Agarwal and R. Ghosh, *Phys. Rev. A* **47**, 1407 (1993).
- [12] M. Graf *et al.*, in *Coherent States: Past, Present and Future*, Proceedings of the International Symposium at Oak Ridge National Laboratory, 1993, edited by D. H. Feng *et al.* (World Scientific, Singapore, 1994).
- [13] P. R. Berman, in *New Trends in Atomic Physics*, edited by G. Grynberg and R. Stora (Elsevier, New York, 1984), p. 451.
- [14] G. Alzetta, A. Gozzini, L. Moi, and G. Orriols, *Nuovo Cimento B* **36**, 5 (1976); G. Alzetta, L. Moi, and G. Orriols, *ibid.* **52**, 205 (1979).
- [15] J.H. Xu, Ph.D. thesis, Scuola Normale Superiore, Pisa, Italy, 1994.